Croatian Society for Materials Protection

Metalurgija/Metallurgy

Vol. 66 No. 2 / 2027

Rigid-Flexible Coupled Dynamic Modeling and Vibration Characteristic Analysis of a Hot Metal Deslagging Robot

Yuhang Zhang [1], Yuqiang Cai [1] and Jingran Zhou [1,*]

https://doi.org/10.64486/m.66.2.5

[1] College of Mechanical Engineering, North China University of Science and Technology, Tangshan, China
* Correspondence: zhoujr@ncst.edu.cn

Type of the Paper: Article
Received: November 27, 2025
Accepted: August 13, 2026

Abstract: Aiming at the mechanical vibration problem caused by the coupling between the flexible deformation of the long-cantilever boom structure and the dynamic characteristics of the gear-rack transmission system during the operation of the hot metal deslagging robot, this paper focuses on conducting a systematic rigid-flexible coupled dynamic modeling and vibration characteristic analysis. By integrating multi-body dynamics and finite element analysis for co-simulation, the dynamic response of the flexible boom during the swinging phase is accurately captured. Furthermore, based on modal coordinate analysis, the vibration generation mechanism and propagation characteristics are revealed.

Keywords: hot metal deslagging robot, rigid-flexible coupled modeling, vibration characteristics

1. Introduction

In the steelmaking process, hot metal pretreatment is a critical step for improving the final steel quality. Among these operations, hot metal deslagging aims to remove the upper slag generated after desulfurization and dephosphorization, and is essential for ensuring the stability of subsequent refining processes and the cleanliness of molten steel [1, 2]. With increasing smelting rhythm and rising quality demands, traditional manual or semi-mechanized deslagging methods can no longer satisfy the requirements of modern steel plants regarding production efficiency, operational safety, and process consistency. Although considerable progress has been made in the optimization of hot metal pretreatment technologies [1–5], automated deslagging based on industrial robots is gradually becoming a key direction in this field [6–10].

However, the operating environment for hot metal deslagging is extremely harsh. Adverse factors such as high-temperature radiation, dust contamination, and heavy-load impacts pose severe challenges to the structural strength, motion accuracy, and long-term reliability of the deslagging robot [11, 12]. Their results indicate that process parameters—including hot metal composition, slag characteristics, and stirring dynamics—directly affect the load characteristics and motion patterns of the deslagging operation, thereby serving as important external sources of vibration excitation. It is noteworthy that the deslagging robot typically employs a long cantilever telescopic boom structure to achieve a large working envelope. Nevertheless, this configuration leads to relatively insufficient system stiffness, which can readily induce significant elastic vibration during heavy-load startup, braking, and variable-speed movements [13].

Therefore, conducting systematic rigid-flexible coupled dynamic modeling and dynamic response analysis has become a key technical issue urgently needing resolution to enhance the performance of deslagging robots

[14, 15]. This study aims to construct an accurate dynamic model that reflects the system's coupling characteristics by integrating multi-body dynamics theory with the finite element analysis (FEA) method. Furthermore, co-simulation technology will be utilized to quantitatively analyze the vibration response, laying a solid theoretical foundation for understanding the essence of vibration and guiding subsequent performance optimization [16]. Different from conventional rigid-body analyses commonly applied to industrial manipulators [17], this study focuses on the vibration mechanism of a hot metal deslagging robot characterized by a long cantilever boom and rack-and-pinion transmission. The contribution of this study lies not only in establishing a rigid-flexible coupled dynamic model, but also in quantitatively characterizing the vibration response and identifying critical operating stages. The proposed model reveals the influence of structural flexibility and transmission-induced nonlinear excitation on end-effector positioning deviation, providing reference data for subsequent vibration suppression and control optimization [18].

2. Dynamics Modeling for the Deslagging Manipulator

The hot metal deslagging robot investigated in this study consists of a base, frame, boom, telescopic arm, hydraulic actuators, and a deslagging tool, as shown in Figure 1. The robot achieves deslagging motion through coordinated rotational and translational joint movements. Among these subsystems, the boom is the primary load-bearing component, characterized by its long cantilever geometry and relatively low stiffness-to-mass ratio. This inherent flexibility makes the boom a critical source of dynamic deformation, and it is therefore treated as a flexible body in the dynamic analysis, whereas all other components are modeled as rigid bodies.

The simplified model of the designed deslagging robot is shown in Figure 1. It primarily comprises core components such as the base, frame, boom, arm, and bucket (deslagging tool). The telescopic movement of the arm is achieved via a rack-and-pinion mechanism engaged with the boom. Structural steel is selected as the primary material for the overall structure.

Before performing the rigid-flexible coupled dynamic simulation, the accuracy of the flexible boom model was verified through a static deformation comparison under gravitational loading. The boom was constrained according to the actual assembly conditions, and its deformation caused by self-weight was calculated using both finite element analysis and theoretical beam theory. Specifically, the maximum vertical deflection at the free end of the boom was selected as the validation indicator. The theoretical deflection was obtained based on the Euler–Bernoulli beam assumption, while the numerical result was extracted from the ANSYS static structural analysis under identical boundary conditions and material properties. The relative deviation between the two methods was less than 5%, indicating that the finite element model can accurately capture the stiffness characteristics of the boom and can subsequently be used for flexible body generation.

After validation, the flexible boom was converted into a Modal Neutral File (MNF) for ADAMS integration. The modal analysis employed mass normalization, where the modal vectors were scaled such that the generalized modal mass matrix became an identity matrix. This normalization process ensured modal decoupling and provided a suitable representation of elastic deformation for rigid-flexible coupled dynamic simulation.

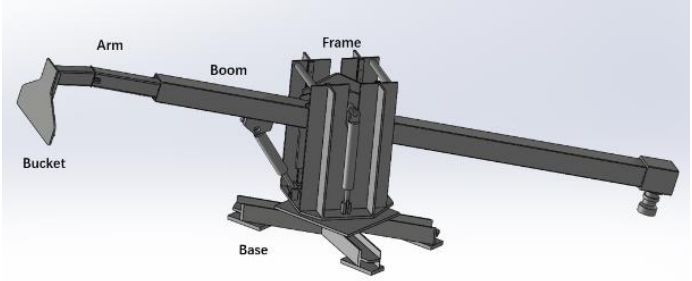


Figure 1. The 3D Model of the Deslagging Robot

https://doi.org/10.64486/m.66.2.5

When establishing a rigid-flexible coupled dynamic model of the deslagging robot with the boom as the flexible component, it is necessary to integrate the kinematics of rigid components with the theory of elastic deformation of flexible bodies. The system equations are formulated using either the Lagrange method or the assumed modes method. The kinetic energy of each rigid body is calculated based on the velocity of the center of mass and the moment of inertia. The total kinetic energy is expressed as:

$$T_R = \frac{1}{2}\sum_{i=1}^{N}(m_i\|v_i\|^2 + \omega_i^T J_i \omega_i) \quad (1)$$

where T_R represents the total kinetic energy of all rigid components; N, the total number of rigid components in the system; m_i, the mass of the i-th rigid component; $\boldsymbol{v}_i$, the velocity vector of the center of mass of the i-th rigid component; J_i, the corresponding inertia; ω_i, the angular velocity vector. The kinetic energy of the flexible body comprises the kinetic energy due to rigid-body motion and the kinetic energy due to elastic deformation.

$$T_F = \frac{1}{2}\int_V \rho\, \dot{R}^T \dot{R}\, dV \quad (2)$$

where ρ is the density of the flexible-body material; R, the position vector of an arbitrary point on the flexible body; $\dot{R}$, the absolute velocity of that point; and V, the volume of the flexible body.

By substituting the velocity expression into the kinetic energy formula and applying finite element discretization, the final expression for the kinetic energy is obtained as:

$$T_F = \frac{1}{2}\begin{bmatrix}\dot{r}\\ \omega\end{bmatrix}^T \begin{bmatrix} mI & -m\tilde{c} \\ m\tilde{c} & J\end{bmatrix}\begin{bmatrix}\dot{r}\\ \omega\end{bmatrix} + \frac{1}{2}\dot{q}_f^T M_{ff}\dot{q}_f + \dot{q}_f^T M_{fr}\begin{bmatrix}\dot{r}\\ \omega\end{bmatrix} \quad (3)$$

where r is the position vector, in the global inertial coordinate system, of the origin of the floating frame of reference attached to the flexible body; $\dot{r}$, the translational velocity vector of the origin of the floating frame of reference; I, the 3 × 3 identity matrix; c, the position vector of the flexible body's center of mass relative to the floating frame of reference, defined in the undeformed state; $\tilde{c}$, the cross product (skew-symmetric) matrix of vector c; $\dot{q}_{f,}$ the modal velocity vector; M_{ff}, the elastic mass matrix; and M_{fr}, the rigid-flexible coupled mass matrix.

The potential energy consists of the gravitational potential energy and the elastic potential energy. The gravitational potential energy is the sum of contributions from the rigid components and the flexible boom's center of mass, while the elastic potential energy is given by:

$$V_{elastic} = \frac{1}{2}u_e^T K_e u_e \quad (4)$$

where u_e is the elastic displacement vector defined in the physical coordinates of the finite element nodes; K_e, the global elastic stiffness matrix.

3. Rigid-Flexible Coupled Model Development

To conduct a co-simulation of the rigid-flexible coupled system of the deslagging robot, the boom must first be converted into a flexible body using ANSYS [19, 20]. The specific procedure involves generating a Modal Neutral File (MNF) for the boom. This file is then imported into the rigid-body model within ADAMS to replace the corresponding boom component. Subsequently, simulation data regarding the vibration conditions during the deslagging process under the rigid-flexible coupled state can be obtained. During the MNF generation process, the finite element physical coordinates are transformed into reduced-order modal coordinates. Since the flexible body is represented by a limited number of retained vibration modes, small numerical residual terms may remain due to modal truncation and numerical precision. These residuals correspond to generalized modal coordinates rather than actual structural deformation and do not affect the prediction of the overall dynamic response of the flexible body. Therefore, the modal responses extracted from the flexible body should be interpreted as vibration characteristics rather than direct measurements of elastic displacement. The

https://doi.org/10.64486/m.66.2.5

generated **MNF file** is read by ADAMS and used to replace the corresponding boom mechanism in the rigid-body model. The detailed workflow of the co-simulation is illustrated in Figure 2.

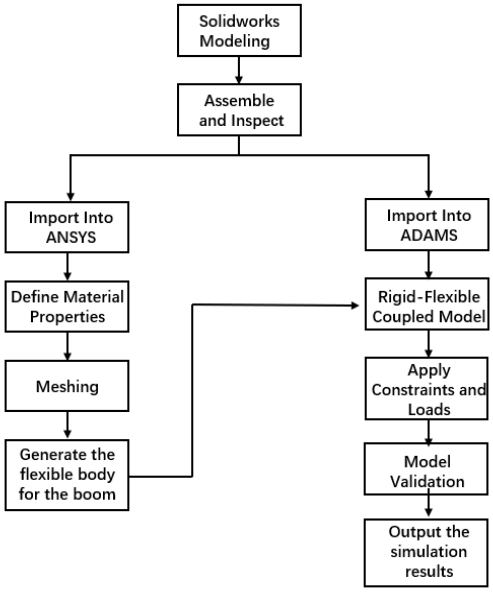


Figure 2. Flowchart of the Co-simulation

The constraint relationships after boom replacement are listed in Table 1.

Table 1. Constraints after Boom Replacement

Constraint Number	Constraint Type	Constrained Bodies
1	Revolute Joint	The front of the boom and the hydraulic cylinder
2	Revolute Joint	The middle of the boom and the hydraulic cylinder
3	Revolute Joint	The boom and the gear

A fixed joint was applied to the base component of the established rigid-body model in ADAMS. A sinusoidal gait was defined at the robot's joints to simulate the motion of the deslagging robot. A measurement point was set at the deslagging tool (bucket). The vibration displacement and velocity variations of each joint and marker point were analyzed using the ADAMS post-processing module. This modeling approach enables simulations that more accurately reflect real-world conditions, thereby facilitating in-depth investigation into vibrations and other issues during the deslagging process. The results provide a model foundation and analytical basis for subsequent research on vibration suppression methods. The rigid-flexible coupled model is shown in Figure 3.



Figure 3. ADAMS-based rigid-flexible coupled dynamic model of the hot metal deslagging robot

https://doi.org/10.64486/m.66.2.5

The theoretical path of the end-effector measurement point on the deslagging robot is generated by the coupled motion of all joints strictly following predefined angular/displacement profiles. However, due to the flexible nature of the boom and the dynamic characteristics of the rack-and-pinion drive (e.g., time-varying meshing stiffness, backlash, and transmission errors), the actual trajectory of the rigid-flexible coupled model exhibits significant positional deviation compared to the desired trajectory of the purely rigid model. This deviation is primarily observed in the Y-Z plane and substantially compromises the precision of the deslagging operation. The following analysis focuses on the vibration profiles at key points:

Before analyzing the end-effector positional deviation, the local dynamic responses at several critical connection points were investigated. Figures 4–7 present the modal coordinate responses extracted from ADAMS at the front joint and middle section of the flexible boom. It should be noted that these values are not the actual elastic deformation of the boom structure. Due to the mass-normalized modal representation used in the MNF file, the extracted generalized coordinates contain numerical residuals with magnitudes on the order of 10^{-7} mm. Such values are physically negligible compared with the actual structural deformation and should not be interpreted as measurable displacement. Instead, these responses are used to identify the periodic excitation characteristics introduced by the rack-and-pinion transmission system.

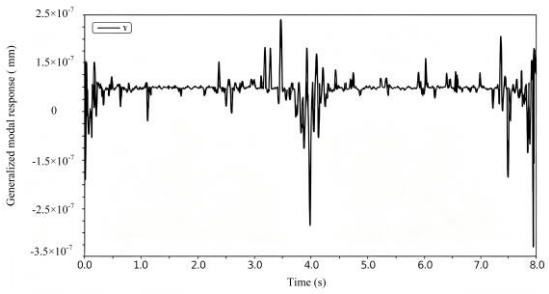


Figure 4. Generalized modal response at the front boom joint along the Y direction

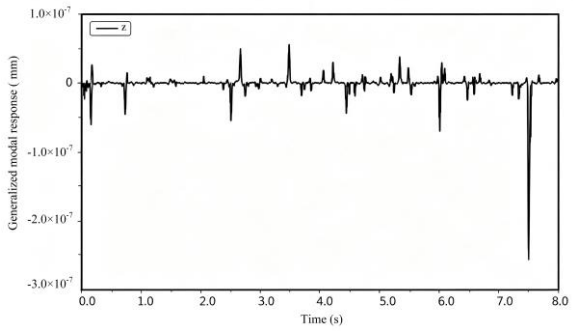


Figure 5. Generalized modal response at the front boom joint along the Z direction

As shown in Figure 4, the vibration profile along the Y-axis at this point exhibits distinct periodic characteristics, which are associated with the rack-and-pinion meshing. Although periodic vibration characteristics are observed, the corresponding values represent generalized modal responses rather than physical displacement and therefore should not be directly interpreted in terms of engineering tolerance. As shown in Figure 5, the vibration amplitude in the Z-direction is relatively smaller than that in the Y-direction, but also demonstrates certain periodic features. This indicates that the front boom joint exhibits a relatively stable dynamic response, although periodic excitation associated with the rack-and-pinion transmission is still present.

https://doi.org/10.64486/m.66.2.5

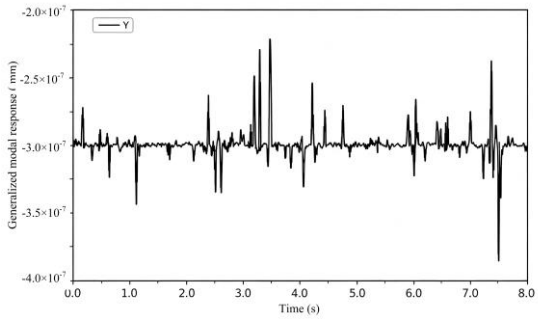


Figure 6. Generalized modal response at the middle boom section along the Y direction

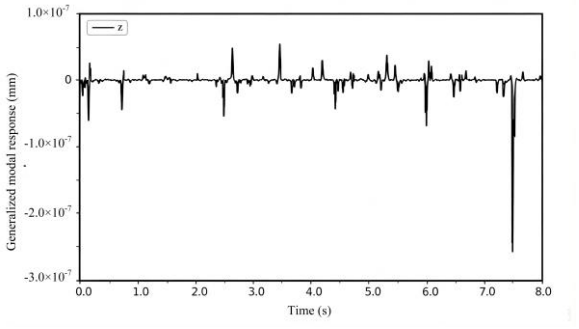


Figure 7. Generalized modal response at the middle boom section along the Z direction

Combining Figures 6 and 7, it can be observed that during the operation of the deslagging robot, the vibration at the midsection of the boom is relatively minor, indicating an overall stable working condition.

The displacement curves of the measurement point at the deslagging tool in the Y-axis direction, Z-axis direction, and the resultant displacement are shown in Figures 8, 9, and 10, respectively.

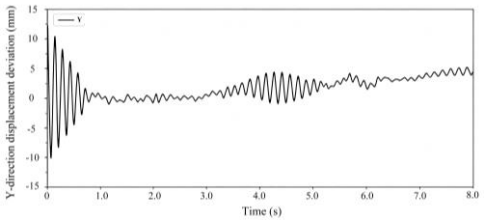


Figure 8. End-effector displacement deviation along the Y direction

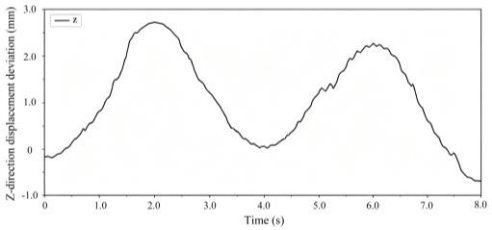


Figure 9. End-effector displacement deviation along the Z direction

The resultant displacement deviation shown in Figure 10 provides an overall evaluation of the spatial positioning error of the deslagging tool. The maximum deviation occurs during the startup stage and reaches approximately 25 mm, while another relatively large deviation appears during the later operation stage. The resultant deviation represents the combined effect of rigid-body motion deviation, elastic deformation of the flexible boom, and drivetrain-induced dynamic excitation. Among these factors, structural flexibility mainly

https://doi.org/10.64486/m.66.2.5

determines the low-frequency deformation characteristics, whereas drivetrain nonlinearities contribute periodic disturbances during motion. The results indicate that the startup process is the most critical operating condition for improving the positioning accuracy of the hot metal deslagging robot. Reducing the acceleration rate, increasing structural stiffness, and improving transmission accuracy are potential approaches for suppressing end-effector deviation.

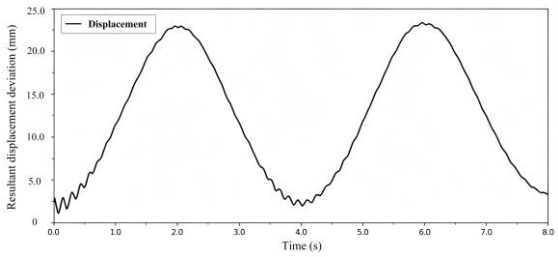


Figure 10. Resultant displacement deviation of the end-effector

As shown in Figure 8, significant vibration error is observed along the Y-axis during the startup phase (0-1 s) and the period of 3-5 s, with a maximum peak value reaching approximately 15 mm. The vibration amplitude decreases thereafter. Figure 9 indicates that a certain level of vibration error also exists in the Z-direction, but its overall magnitude is smaller than that in the Y-direction. The resultant displacement curve, shown in Figure 10, comprehensively reflects the spatial position deviation of the end-effector. The most severe vibration occurs during the 0-1 s startup phase, with a peak value of about 25 mm. A smaller peak (approximately 17 mm) also appears during the 3.5-4.5 s period. Subsequently, the curve tends to stabilize relatively, though fluctuations persist.

Structural flexibility mainly contributes to low-frequency deformation caused by gravity and inertial loading, whereas transmission nonlinearities introduce periodic excitation associated with rack–pinion engagement. Their coupling effect becomes most significant during startup due to rapid acceleration.

4. Conclusion

In this study, a rigid-flexible coupled dynamic model was developed to investigate the vibration characteristics and positioning deviation mechanism of a hot metal deslagging robot by considering the elastic deformation of the long-cantilever boom and the dynamic excitation from the rack-and-pinion transmission system. The model was established by integrating finite element modal analysis with ADAMS multibody dynamics, enabling the interaction between structural flexibility and drivetrain excitation to be effectively captured.

The simulation results demonstrate that the coupling effect between boom deformation and transmission-induced excitation significantly influences the dynamic performance of the deslagging robot. The startup stage is identified as the most critical operating condition, where rapid acceleration excites the flexible modes of the boom and produces the maximum dynamic response. The end-effector positioning deviation results show that structural flexibility mainly determines the overall deformation trend, while drivetrain nonlinearities introduce periodic dynamic fluctuations. The resultant displacement deviation from the ideal rigid-body trajectory confirms the necessity of rigid-flexible coupled modeling for accurate dynamic evaluation.

The obtained dynamic response characteristics and positioning error data provide a theoretical basis for vibration suppression, structural optimization, and subsequent controller design of hot metal deslagging robots.

Acknowledgments

This work was supported by the Tangshan Municipal Science and Technology Planning Project (24130218c).

 https://doi.org/10.64486/m.66.2.5

References

[1] J. Ji, H. Du, Y. Jiang, D. Li, and S. Zhang, "Effect of impellers on particle mixing behaviour in KR desulphurization process," *Ironmaking & Steelmaking*, vol. 49, no. 2, pp. 167–177, Feb. 2022, https://doi.org/10.1080/03019233.2021.1972740

[2] H. Negishi, Y. Uchida, and R. Kawabata, "Complete Hot-recycling Technique of Dephosphorization Slag for Hot Metal Pretreatment with Converter," *ISIJ International*, vol. 65, no. 11, pp. 1642–1652, 2025, https://doi.org/10.2355/isijinternational.ISIJINT-2025-248

[3] Z. Shi, W. Lv, and G. Mei, "A novel soft sensing modelling approach for sulphur content estimation in hot metal pretreatment process," *Ironmaking & Steelmaking*, vol. 51, no. 6, pp. 579–596, Aug. 2024, https://doi.org/10.1177/03019233241247383

[4] Z. Zhao, X. Feng, Y. Zhang, Y. Zhang, and Y. Wu, "Development of Solid Waste-Based Composite Calcium Ferrite Flux and Its Application in Hot Metal Pre-Dephosphorization," *Materials*, vol. 17, no. 5, Art. no. 992, Jan. 2024, https://doi.org/10.3390/ma17050992

[5] Y. Zhao, L. Zhang, W. Chen, S. Cheng, and Y. Ren, "Kinetic modeling on hot metal desulfurization with mechanical stirring," *J. Iron Steel Res. Int.*, vol. 29, no. 5, pp. 719–724, May 2022, https://doi.org/10.1007/s42243-022-00764-w

[6] J.-S. Kim, G.-T. Ahn, and S.-Y. Park, "Estimation of Slag Removal Path using CNN-based Path Probability of Ladle Image Blocks," *Int. J. Control Autom. Syst.*, vol. 18, no. 3, pp. 791–800, Mar. 2020, https://doi.org/10.1007/s12555-019-0019-3

[7] J. Lee, G.-T. Ahn, and S.-Y. Park, "Slag Removal Path Estimation by Slag Distribution Image and Multi-Task Deep Learning Network," *IEEE Access*, vol. 9, pp. 118541–118552, 2021, https://doi.org/10.1109/ACCESS.2021.3107677

[8] W. Long, J. Zheng, H. Yu, M. Ding, and J. Li, "Image-Based Iron Slag Segmentation via Graph Convolutional Networks," *Complexity*, vol. 2021, Art. no. 6691117, 2021, https://doi.org/10.1155/2021/6691117

[9] J. Wu and D. Xu, "Semi-solid metal oxide slag morphology detection based on cross-modal learning," *Engineering Applications of Artificial Intelligence*, vol. 173, Art. no. 114380, Jun. 2026, https://doi.org/10.1016/j.engappai.2026.114380

[10] D. Xu, Y. Xiao, J. Liu, and Y. Guo, "Decouple visual servoing of slag removal robots based on vanishing point," *Applied Mathematical Modelling*, vol. 152, Art. no. 116585, Apr. 2026, https://doi.org/10.1016/j.apm.2025.116585

[11] J. H. Peng, X. W. Cheng, J. Wang, and L. C. Xiao, "Analysis of temperature field and thermal stress of molten iron slagging-off robot arm," *Metalurgija*, vol. 63, no. 1, pp. 25–27, Jan. 2024

[12] F. Zhang and Z. Yuan, "The Study of Coupling Dynamics Modeling and Characteristic Analysis for Flexible Robots with Nonlinear and Frictional Joints," *Arab J Sci Eng*, vol. 47, no. 12, pp. 15347–15363, Dec. 2022, https://doi.org/10.1007/s13369-022-06581-3

[13] D. Liang, M. Cui, S. Li, B. Chang, Z. Wang, and J. Zhang, "Rigid-flexible coupling dynamic modeling and adaptive intelligent composite control for a novel redundantly actuated flexible parallel robot," *Advances in Engineering Software*, vol. 212, Art. no. 104048, Jan. 2026, https://doi.org/10.1016/j.advengsoft.2025.104048

[14] Y. Guo *et al.*, "Strong, Recyclable, Bio-Based Vitrimers by Tailored Rigid-Flexible Structures for Advanced Carbon Fiber-Reinforced Polymers," *Advanced Science*, vol. 13, no. 3, Art. no. e13935, Jan. 2026, https://doi.org/10.1002/advs.202513935

[15] L. Wu and Q. Wu, "An Adaptive Grasping Multi-Degree-of-Freedom Prosthetic Hand with a Rigid–Flexible Coupling Structure," *Sensors*, vol. 25, no. 19, Art. no. 6034, Jan. 2025, https://doi.org/10.3390/s25196034

[16] Z. Deng, H. Pang, and H. Fang, "Dynamic modeling of a modular worm-like robot with rigid–flexible coupled structure," *J. Phys.: Conf. Ser.*, vol. 3133, no. 1, Art. no. 012012, Oct. 2025, https://doi.org/10.1088/1742-6596/3133/1/012012

[17] G. Cui, B. Li, W. Tian, W. Liao, and W. Zhao, "Dynamic modeling and vibration prediction of an industrial robot in manufacturing," *Applied Mathematical Modelling*, vol. 105, pp. 114–136, May 2022, https://doi.org/10.1016/j.apm.2021.12.031

[18] J. Yang, F. Meng, X. Wang, and H. Song, "Motion-dependent modal analysis of flexible-joint mechanisms," *Journal of Sound and Vibration*, vol. 619, Art. no. 119416, Dec. 2025, https://doi.org/10.1016/j.jsv.2025.119416

[19] L. Du, N. L. Lu, and P. Lan, "Analysis of Flexibility and Stability of Crane Telescopic Boom with Elastic Restraint and Second-Order Effect," *Advanced Materials Research*, vol. 774–776, pp. 109–113, 2013, https://doi.org/10.4028/www.scientific.net/AMR.774-776.109

[20] A. Trąbka, "Dynamics of telescopic cranes with flexible structural components," *International Journal of Mechanical Sciences*, vol. 88, pp. 162–174, Nov. 2014, https://doi.org/10.1016/j.ijmecsci.2014.07.009